

# The Star Formation History of the Hubble Sequence: Spatially Resolved Colour Distributions of Intermediate Redshift Galaxies in the Hubble Deep Field

R. G. Abraham<sup>1,2</sup>, R. S. Ellis<sup>2</sup>, A. C. Fabian<sup>2</sup>, N. R. Tanvir<sup>2</sup>, and K. Glazebrook<sup>3</sup>

<sup>1</sup>*Royal Greenwich Observatory, Madingley Road, Cambridge, CB3 0EZ*

<sup>2</sup>*Institute of Astronomy, University of Cambridge, Madingley Road, Cambridge CB3 0HA*

<sup>3</sup>*Anglo-Australian Observatory, P. O. Box 296, Epping, NSW 2121, Australia*

Received: Accepted:

## ABSTRACT

We analyse the spatially resolved colours of distant galaxies of known redshift in the Hubble Deep Field, using a new technique based on matching resolved four-band colour data to the predictions of evolutionary synthesis models. Given some simplifying assumptions we demonstrate how our technique is capable of probing the evolutionary history of high redshift systems noting the specific advantage of observing galaxies at an epoch closer to the time of their formation. We quantify the relative age, dispersion in age, ongoing star-formation rate, and star-formation history of distinct components. We explicitly test for the presence of dust and quantify its effect on our conclusions. To demonstrate the potential of the method, we study the near-complete sample of 32  $I_{814} < 21.9$  mag galaxies with  $\bar{z} \sim 0.5$  studied by Bouwens et al (1997). The dispersion of the internal colours of a sample of  $0.4 < z < 1$  early-type field galaxies in the HDF indicates that  $\sim 40\%$  [4/11] show evidence of star formation which must have occurred within the past third of their ages at the epoch of observation. This result contrasts with that derived for HST-selected ellipticals in distant rich clusters and is largely independent of assumptions with regard to metallicity. For a sample of well-defined spirals, we similarly exploit the dispersion in colour to analyse the relative histories of bulge and disc stars, in order to resolve the current controversy regarding the ages of galactic bulges. Dust and metallicity gradients are ruled out as major contributors to the colour dispersions we observe in these systems. The median ages of bulge stars are found to be significantly older than those in galactic discs, and exhibit markedly different star-formation histories. This result is inconsistent with a secular growth of bulges from disc instabilities, but consistent with gradual disc formation by accretion of gas onto bulges, as predicted by hierarchical theories. We extend our technique in order to discuss the star formation history of the entire Bouwens et al sample in the context of earlier studies concerned with global star formation histories. Finally, we consider how to extend our method using near-infrared data and to deeper samples.

**Key words:**

## 1 INTRODUCTION

The public availability of the Hubble Deep Field (HDF, Williams et al 1996) has led to a surge of progress in our understanding of the faint galaxy population. The flatter slope ( $d \log N / dm$ ) of the optical counts beyond  $B \simeq 25$  mag found from earlier deep ground-based studies (Lilly et al 1991, Metcalfe et al 1995, Smail et al 1995) has been confirmed from the HDF data. This flat slope, when combined with the relative paucity of  $U$ -dropouts (which confirms that most of even the faintest optical sources have  $z < 3$

[Guhathakurta et al 1990, Lanzetta et al 1996, Connolly et al 1997]), implies the bulk of the extragalactic background light must have been produced at a relatively low redshift (Ellis 1997).

The HDF has also contributed much to our understanding of distant galaxy morphology. Various authors (Abraham et al 1996a; Mobasher et al 1996; Odewahn et al 1996; Driver et al 1998) have used the HDF to extend the earlier Medium Deep Survey morphological source counts (Glazebrook et al 1995; Driver et al 1995; Abraham et al 1996b) to fainter

limits, finding a surprisingly high fraction of the  $I_{814} < 25$  mag sources cannot be categorised within the Hubble sequence of regular systems. A key question is the physical nature of these sources and their present-day counterparts. Another striking result from the HDF is the small angular sizes of the faintest sources, implying physical extents of only 2-4  $h^{-1}$  kpc. In a recent analysis, Bouwens et al (1997) suggest that such sizes cannot be reconciled with the expected redshift and surface brightness dimming of typical  $z < 1$  sources and thus claim substantial physical growth and merging must have occurred for the galaxy population during the redshift range  $1 < z < 3$ . The deep HDF data complement recent morphological studies by Brinchmann et al (1998), Lilly et al (1998) and Schade et al (1998) who have analysed the joint morphological-spectroscopic data obtained from a HST imaging survey of a subset of CFRS (Lilly et al 1995) and LDSS (Ellis et al 1996) redshift surveys. They find strong evolutionary trends in a population of  $z < 1$  galaxies with irregular morphology but only modest changes in the abundance of large regular disc and spheroidal galaxies. It is not clear whether these trends are consistent with semi-analytical models based on hierarchical growth (Baugh, Cole & Frenk 1996). For there to be a peak of star formation activity at  $z \simeq 1-2$  (Madau 1997), either the evolutionary behaviour of massive regular galaxies beyond  $z \simeq 1$  must change dramatically from that observed for  $z < 1$ , or perhaps the trends delineated from the optical photometric data are underestimated because of complications such as dust extinction (Meurer et al 1997).

Another important aspect of the Hubble Deep Field is the ultra-deep spectroscopic follow-up survey work undertaken with the Keck telescopes (Cowie 1997, Lowenthal et al 1997, Cohen et al 1996). These surveys have confirmed the conclusions suggested by the photometric analyses above and raised confidence in the validity of photometric redshifts estimated from multicolour photometry alone (Ellis 1997, Hogg et al 1998).

In this paper we wish to explore a new approach to the HDF data, somewhat related to the photometric redshift technique, but which exploits the true benefit of HST, namely its ability to *resolve* distant galaxies. Rather than use the multicolour data to predict redshifts for distant sources, we instead explore the *resolved multicolour data for galaxies of known redshift* using spectral-synthesis models. For galaxies with  $\bar{z} \simeq 1$ , the 4-filter HDF colours are dominated by main sequence stars whose turn-off ages are less than 4-5 Gyr. As the evolutionary history of such stars is well-understood, modulo the usual assumptions concerning the stellar initial mass function and chemical composition, the multicolour HDF data can be used to derive relative ages for physically distinct components of distant galaxies, test for the presence of dust and possibly address the puzzling nature of the irregular sources which appear with such abundance.

This paper is primarily concerned with an initial application of our technique to a well-defined population of  $I_{814} < 21.9$  mag galaxies with redshifts drawn from Bouwens et al (1997). This sample constitutes the faintest statistically-complete spectroscopic redshift sample currently available in the HDF. The use of this sample has the benefits that (a) conclusions drawn from it can be compared to those of independent studies sampling the same magnitude and redshift

range (e.g. Brinchmann et al 1997); and (b) by restricting our sample to relatively bright limits and moderate redshifts ( $\bar{z}=0.5$ ), we are working with galaxies that are well-resolved and can be described within the traditional framework of the Hubble System. The scientific focus of the present paper is directed towards a better understanding of two contentious yet fundamental issues central to the origin of the Hubble classification sequence: the relative ages of bulges and discs, and the formation history of elliptical galaxies. We will also use our synthesis results to place some constraints on the previous appearance of our galaxy sample.

In our own Galaxy the observational evidence for early bulge formation seems established, mainly since the main tracers of bulge/halo populations (eg. globular clusters and RR Lyrae stars) are known to be old. The notion that bulges form well before the discs in the first stage of galactic collapse is the essential component in both the original ELS scenario (Eggen, Lynden-Bell, & Sandage 1962) and more modern variants (eg. Carney et al. 1990). Hierarchical galaxy formation scenarios also require old bulges formed by mergers (eg. Kauffmann, White, & Guiderdoni 1993; Baugh, Cole & Frenk 1996), with visible discs built-up gradually from gas accreted onto these merger remnants. Recently, however, the issue of the relative age of the bulge and disc in extragalactic systems has become controversial. N-body simulations indicate that bulges form naturally from bar instabilities in discs (Norman, Sellwood, & Hassan 1996; Combes et al. 1990), and recent observations now seem to indicate that bulges display the morphological and dynamical characteristics of such a formation scenario (eg. triaxiality or ‘‘peanut’’ shapes (Kuijken & Merrifield 1995), cylindrical rotation (Shaw 1993), and disky kinematics (Kormendy 1992). On the basis of model fits, de Jong (1996) concludes that age is likely to be a dominant contributor to color gradients in local spirals. However extrapolation of colour gradients to the inner parts of the galaxies suggests that at least the inner discs *cannot be distinguished in terms of colour* from bulges (Balcells & Peletier 1994; de Jong 1996). This is perhaps somewhat surprising given the visual impression from ‘‘true colour’’ HST images of distant galaxies, in which bulges seem generally redder than disks even at quite small galactocentric radii (van den Bergh et al. 1996).

In another recent challenge of what had, hitherto, been regarded as a well-established viewpoint, Kauffmann et al (1996) and Zepf (1997) have introduced the possibility that elliptical galaxies are continuously formed from merging systems as expected in hierarchical models for the growth of structure, rather than formed at high redshift in a single burst of star formation (c.f. Baade 1957). The observational evidence supporting the ‘traditional’ view was based primarily on the small scatter in the colour-magnitude diagram of cluster ellipticals (Sandage & Visvanathan 1978, Bower et al 1992). This test has also been extended to higher redshift cluster samples with morphological classifications from HST (Ellis et al 1997, Stanford et al 1998).

Unfortunately, as Kauffmann (1996) points out, cluster samples are ill-suited to testing the hierarchical picture as they represent accelerated regions so far as structure growth is concerned. It is quite possible that most of the rich cluster ellipticals are truly old as their homogeneously distributed colours imply. The ultimate test of Kauffmann et al’s conjecture lies in the analysis of ellipticals in field samples. The

currently-available samples are too small for robust results (Schade et al 1998) although Zepf (1997) claims the absence of red objects at very faint limits in the HDF is consistent with hierarchical predictions. Glazebrook et al (1998) have also claimed evidence for younger field ellipticals in data from the Medium Deep Survey, on the basis of  $I-K$  colours.

A plan of the paper follows. In §2 we introduce the principles of our method for analysing spatially-resolved multi-colour data, and outline the basic assumptions and the uncertainties associated with the technique. In §3 we illustrate how the method works by analysing multicolour data for 3 HDF galaxies of known redshift. In §4 we introduce the Bouwens et al sample and discuss its salient properties in the context of earlier morphological studies. We partition the sample into sources of ellipticals and spirals and explore the history of star formation for both types. Utilising the statistical completeness of the Bouwens et al sample, we use our derived star formation rates to calculate contributions to the volume averaged values and predict the recent past appearance of the various classes. In §5 we discuss our method more generally and explore briefly the prospects for validating our results and extending the work to higher redshift systems. In §6, we summarise our main results. Unless stated otherwise, throughout this paper our adopted cosmology is one where  $H_0 = 70 \text{ km s}^{-1} \text{ Mpc}^{-1}$ ,  $\Omega = 0.2$ , and  $\Lambda = 0$ .

## 2 METHODOLOGY

In general terms any age-dating of galaxies using broad-band photometry is affected by numerous complications including the age-metallicity degeneracy, possible effects of internal dust extinction and variations in the stellar initial mass function (see Renzini 1995 for a review). However the crucial advantage of resolved colour analyses is that they make possible studies of *relative* age and star-formation history of the components within galaxies, which as we will show are far more robust than absolute ages based upon integrated colours. Furthermore, in the case of HDF galaxies, the significant look-back time to the distant sources selected for study means that age uncertainties have far less of an effect than would be the case in analysing the history of local stellar populations. *Our approach will thus be to focus more on the relative age distributions of stellar populations internal to galaxies of a given morphological type, rather than attempting to determine absolute ages.* By weighting component age distributions with their stellar luminosities we hope to address more general questions such as the recent ( $<5$  Gyr) star formation history of disc and spheroidal components. This is an important goal since, at  $z \simeq 0.5$ , the previous 5 Gyr spans the important redshift range  $z < 2.5$ .

To understand how 4-filter colour data can be used to place constraints on past star formation history, consider first a late-type spiral whose star formation history can be approximated by a constant star-formation rate. In reality the constant SFR is effectively a time-average over the appearance and disappearance of spatially distinct star forming regions, each of which can be considered as a simple stellar population with a lifetime (before disruption or gas depletion) which is short compared to the dynamical timescale of the galaxy. Over time these young populations gradually mix with older generations of stars and assimilate into older

galactic components. We will translate this qualitative picture for galaxy evolution into the quantitative language of spectral synthesis modelling (Charlot & Bruzual 1991).

The emergent flux from a composite stellar system,  $F_\lambda$ , at time  $t$  can be represented by the convolution of the spectrum of an evolving instantaneous starburst,  $f_\lambda(x)$  with an assumed star-formation rate (SFR) function  $\Psi(t)$ :

$$F_\lambda(t) = \int_0^t \Psi(t-x)f_\lambda(x)dx \quad (1)$$

$f_\lambda(t)$  term is known given a stellar initial mass function (IMF) and metallicity from libraries of template stellar spectra and evolutionary isochrones. For a given star-formation history an age track can be constructed on a colour-colour diagram using Equation 1. When treating galaxies as point sources the integrated colours define a single position on a colour-colour diagram, and given the uncertainties in the assumed values for  $\Psi(t)$ , the IMF and metallicity, unique stellar ages cannot be derived.

Since galaxies are not generally homogenous systems with a single age and star-formation history, *when they are spatially resolved we can expect a dispersion of points on colour-colour diagrams.* The important point we explore in this paper is whether the nature of this dispersion can be used to overcome many of the ambiguities inherent in Equation 1. For example, the distribution of pixel by pixel colours within a galaxy image is a record of the manner in which the stellar population has been assembled (eg. via numerous small bursts, or by a smaller number of larger bursts). We expect resolved sites of active star formation to approximate instantaneous starbursts and therefore  $\Psi(t)$  to be a  $\delta$ -function, effectively breaking the convolution degeneracy in Equation 1. In practice, therefore, the distribution of pixel colours should directly trace the shape of  $f_\lambda$  for a set of ages.

### 2.1 Colour-colour Predictions

Model colour-colour age tracks for the HDF filter set were computed using the GISEL96 spectral synthesis code of Charlot & Bruzual (1991;1996;1998). For convenience, in our modelling, we assumed a Salpeter initial mass function (IMF) with low and high mass cut-offs of  $0.1 M_\odot$  and  $125 M_\odot$  respectively (this latter cut-off is fixed in the standard GISEL96 distribution). We also assumed that the colours of individual pixels can be modelled using exponential star-formation histories with characteristic timescale  $\tau$ , ie.  $\Psi(t) = \Psi_0 e^{(-t/\tau)}$ , which is often used to model the integrated colours of galaxies (Kennicutt 1991). This allows a fairly generic parameterization of the star formation history, since as  $\tau \rightarrow \infty$  this model approximates constant star formation, while  $\tau \rightarrow 0$  approximates an instantaneous burst. This exponential form is clearly an important assumption, but we would like to emphasize two points. Firstly, if the assumed form is correct then we expect the dispersion in galaxy colours to scatter along the predictions of exponential  $\Psi(t)$  tracks, which is in fact generally seen in our data. The second point is that exponential star formation histories for individual pixels *do not* necessarily result in a global exponential star-formation history for the galaxy considered as a whole (ie. when the total light from all pixels is superposed), unless the galaxy is coeval with a universal star-formation history applying to all pixels.

Representative colour-colour tracks for stellar populations seen at various redshifts with different assumed star formation histories and metallicities are shown in Figure 1. Arrows at the corners of the panels illustrate the effects of foreground-screen dust extinction in the host galaxy with rest-frame value  $E_{B-V} = 0.1$  mag, assuming Galactic, SMC, and local starburst extinction curves (Pei 1992, Calzetti 1997). Taken together, the panels in this figure illustrate how the colour-colour tracks change as the result of varying the star-formation timescale, dust content, and metallicity of the models.

The colour vs. age tracks on the colour-colour diagrams,  $c(t)$ , have four free parameters: age  $t$ , star formation history e-folding timescale  $\tau$ , metallicity  $Z$ , and dust extinction  $E_{B-V}$  (parameterized in terms of relative optical extinction in the rest frame), i.e.  $c(t)$  is shorthand for  $c(t, \tau, Z, E_{B-V})$ . Prior to fitting pixel-by-pixel colours to these models, all galaxy images were re-registered to sub-pixel accuracy. This was accomplished by calculating offsets between the different bands (in the version 2 stacked images provided by STScI) by cross correlating the images, and then resampling to remove the subpixel positioning errors with spline interpolation.

For each pixel in the galaxy image, we compute the optimum evolutionary track using a maximum likelihood estimator  $\mathcal{L}$  that is effectively least-squares:

$$\mathcal{L}(t, \tau, Z, E_{B-V}) = \prod_{n=1}^4 \frac{1}{\sqrt{2\pi}\Delta C_n} \exp\left(-\frac{(c_n - C_n)^2}{2\Delta C_n^2}\right) \quad (2)$$

where the product is over the four colours, and  $[C_n, \Delta C_n]$  are the data colours and errors in the pixel (determined using the formulae in Williams et al. 1996). Appropriate ranges to maximise the likelihood within were determined from simple astrophysical constraints. In the next section we describe these astrophysical constraints, and describe in a general way the effects of varying the model parameters.

## 2.2 Qualitative Properties of the Models

### 2.2.1 Star-formation History

Unsurprisingly, Figure 1 indicates that the exponential star-formation timescale  $\tau$  (which will be given in units of Gyr throughout this paper) is the dominant parameter controlling the colour of an evolving stellar population (Tinsley 1980). The separation between the tracks for the HDF filter set is most pronounced for redshifts  $z > 0.3$ , so the techniques described in the present paper are optimized for non-local galaxies when using the HDF filter set. As expected, tracks corresponding to large values of  $\tau$  (effectively constant star-formation) predict roughly constant colour indices at all ages for all redshifts. Greater trends are seen for evolving populations with decreasing star-formation timescales.

For models with long and short  $\tau$ , our sensitivity to the past history becomes less precise. Clearly the evolution in colour is greatest over intermediate values of  $\tau$ , and over ages corresponding to the main sequence lifetimes sampled in the HDF filter set. In practice, the colours are not very sensitive to age changes beyond 5 Gyr. For local samples this is a major deficiency in understanding the history of galaxy formation (Bower et al 1992). However, at a look-back time

corresponding to  $\bar{z} \simeq 0.5$ , the range in stellar ages probed is particularly useful if, as seems likely, the bulk of the star formation in the Universe occurred at  $z \simeq 1.5$  (Madau et al 1997).

At the other extreme, as  $\tau$  approaches 100 Myr, the tracks also become degenerate as  $\tau$  becomes comparable with the main-sequence lifetimes of the massive stars which dominate the rest-frame ultraviolet flux. This is an important characteristic implying that those populations evolving with timescales  $\tau \sim 10^8$  years move along tracks similar in shape to those of individual star clusters whose formation timescales are  $\tau \simeq 10^{4-5}$  years; in practice the evolution of star clusters can be modeled as instantaneous starbursts, cf. Meurer et al. 1995. However an effective lower limit on  $\tau$  is imposed by the resolution of HST, since the WFPC-2 pixel size of  $0.1''$  corresponds to  $\sim 1$  kpc at  $z \sim 1$  and thus individual star-clusters are not resolved. The effective limit is given by the speed at which information can travel across a resolution element. Making the conservative assumption that information from shocks and winds within a star-formation complex propagates along the IGM at speeds  $< 0.01c$  over distances  $> 1$  kpc, in the present paper we adopt a minimum timescale of  $\tau = 5 \times 10^7$  years. Therefore, for the maximum likelihood analysis in this paper we explored the range  $0.05 < \tau < 3$  Gyr, sampled finely at intervals  $\delta\tau = 0.1$  Gyr.

### 2.2.2 Dust

The three extinction laws adopted in Figure 1 predict markedly different dust vectors<sup>\*</sup>. Because of this, a strong variation in galaxian internal colour originating mostly from dust extinction, as opposed to age, is difficult to rule out in any individual object. Indeed, it is usually the case that for any individual galaxy an appropriate combination of attenuation strength and extinction law can be chosen in order for dust obscuration to mimic the colour variations predicted by a range in ages. Fortunately, this is not true for our galaxy samples considered as a whole because a general ‘‘dust-age degeneracy’’ would require fine-tuning in the choice of extinction law and attenuation strength as a function of redshift. We might also assume that any dust present in distant galaxies would be distributed similarly to that in local systems, at least for systems with regular appearance. If, as is the case locally, dust is not distributed uniformly on scales larger than a few kiloparsecs, then for pixels corresponding to physically large features, scatter in the colours along the direction of predicted dust vectors might be taken as a sign of extinction, while uniform colours can be taken as a sign of generally low dust content. Since (as will be shown) the scatter in the internal colours of the galaxies studied in this paper is mostly along the predicted age tracks, dust is likely to be playing a subsidiary role in defining the internal galaxian colours. (The availability of both  $U_{300}$  and  $B_{450}$

<sup>\*</sup> This is partly because local extinctions curves are differentiated mainly in terms of degree of ultraviolet extinction, and partly because the 2175Å dust feature (prominent in the Galactic extinction curve) shifts into the bluer HDF filter bandpasses at moderate redshifts.

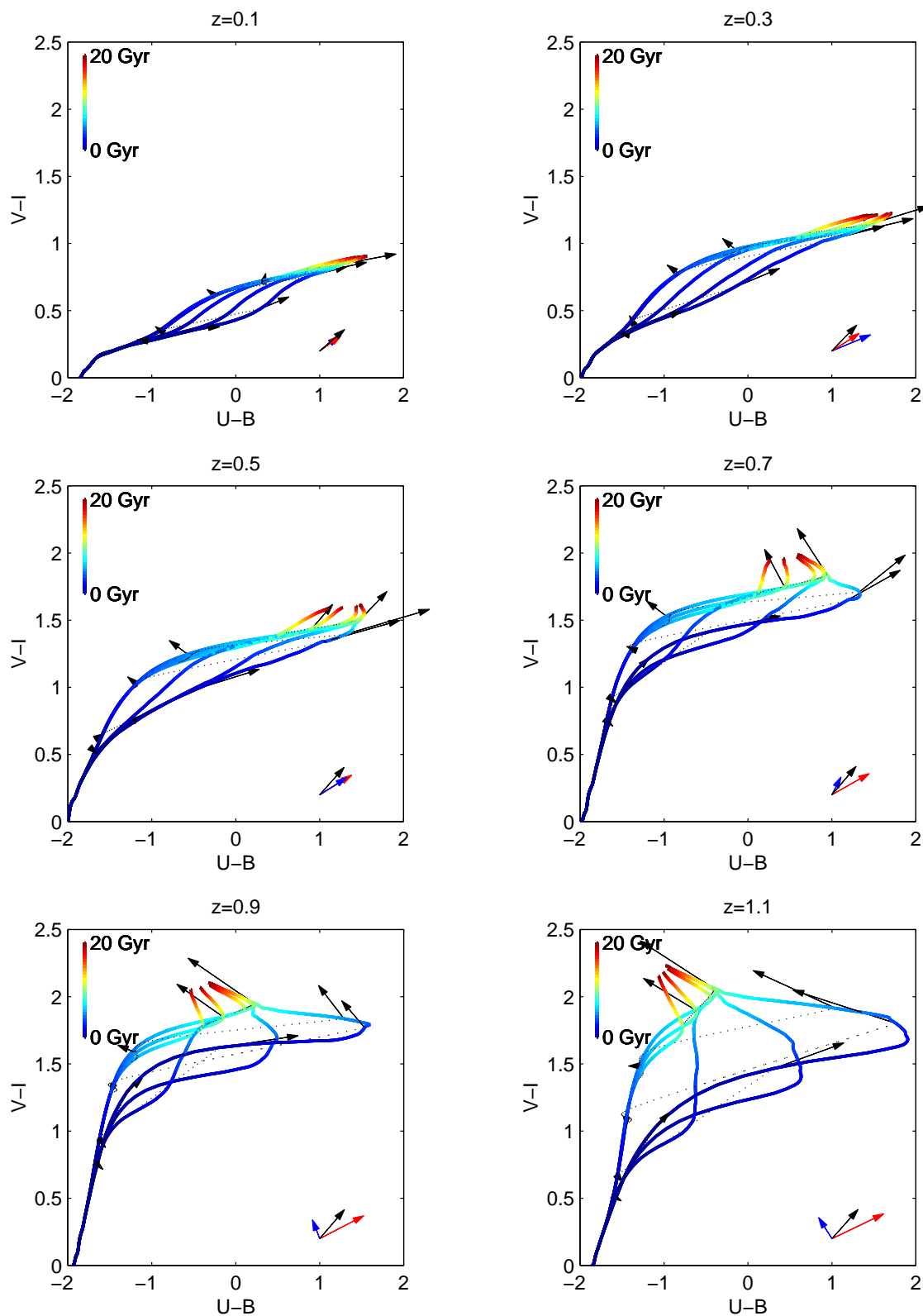


**Figure 1.** Age tracks on the HDF  $V-I$  vs.  $U-B$  colour colour plane for model galaxies viewed at various redshifts. The age (time from the first star formation to the epoch of observation) is indicated by the coloured bar in the left corner. The model tracks show exponentially-decaying star formation histories corresponding to timescales  $\tau$  (Gyr) = 0.2, 0.5, 0.8, 1.1, 1.4, 1.7. Dotted lines connect points at equal ages on the tracks. Arrows on the tracks indicate the effect of changing metallicities from 30% solar to solar. Arrows with a common origin at the bottom-right of each panel are vectors indicating the effect of reddening in the host galaxy. Rest-frame reddening of  $E_{B-V} = 0.1$  mag for Galactic (blue arrow), SMC (red arrow), and Calzetti (1997) local starburst extinction curves (black arrow) are shown. See text for further details.

provides an important constraint given the significant redshifts for most of our galaxies, and the sharply rising dust extinction in the UV.)

In addition to these general considerations which apply to the sample as a whole, we have also chosen to incorporate dust explicitly as a free parameter in our maximum-likelihood analysis, using the extinction law of Calzetti (1997). We chose to consider only the single Calzetti law in our maximum-likelihood analysis as a compromise between choosing to neglect dust completely, which we felt to be rather unrealistic in spite of the general considerations described earlier, and choosing to allow complete freedom in the choice of extinction law, which would enormously complicate the analysis. In the future more solid constraints on the dust content (and appropriate extinction law) may be obtained by augmenting the star-formation histories inferred from the present analysis with integrated *JHK* and *H + K*-band fluxes (Cowie 1997, Dickinson et al 1998) or their resolved equivalents using NICMOS. Future data may also help to constrain the geometry of the dust extinction. The present paper assumes extinction can be modelled using a patchy foreground screen, which we adopted purely for the sake of simplicity, although it should also be noted that Calzetti (1997) argues that a foreground screen model gives a somewhat better representation of the extinction in starburst galaxies than does a mixed dust model.

### 2.2.3 Chemical Enrichment

The age-metallicity degeneracy that is a common characteristic of colour-colour diagrams for early-type galaxies and globular clusters is evident in the tracks shown in Figure 1. In the context of the present paper, where many of the stellar populations being studied are rather young, the degeneracy is less troublesome. For young populations studied in the rest-frame UV, the observable light is dominated by luminous stars at the high mass end of the IMF. Such stars are less sensitive to metallicity variations (as seen in Figure 1) and thus, for the first few Gyr, modest metallicity variations cannot mask a large range in ages.

For ages  $t > 3$  Gyr metallicity gradients *can* in principle play an important role in defining the internal colours of galaxies. In addition, although our synthesis models do incorporate post-MS contributions, it is possible that a UV excess attributed by us to younger stellar populations could represent some deficiency in the treatment of post-MS phases as has been the case for nearby ellipticals (Charlot, Worthey, & Bressan 1996). As was the case with local data, however, the spatial resolution of the UV light is a key discriminant between young and old stellar populations.

Throughout the remainder of this paper we will explore metallicity variations by restricting consideration to a fixed set of metallicities appropriate for local Hubble sequence galaxies: 30% Solar, Solar, and 150% Solar.

## 2.3 Key Assumptions

In summary, our methodology is based on three key assumptions: (1) GISSEL96 models with exponential star formation histories accurately model the colours of individual pixels on galaxy images. (2) Dust extinction can be parameterized

by patchy foreground screen extinction using the Calzetti (1997) dust law. (3) Metallicity lies in the range 30% Solar - 150% Solar.

The first assumption can be justified internally from the data given the qualitatively good agreement between the scatter in pixel-by-pixel colours and the shapes of exponential star formation history tracks. The agreement between this dispersion and the models also suggest that dust plays a subsidiary role in the distribution of galaxian internal colours (at least at the moderate redshifts explored in this paper), although no attempt will be made to constrain the detailed form of the dust law from our data. The final assumption simply corresponds to metallicity lying within a reasonable large range of values representative of those seen in local Hubble sequence galaxies.

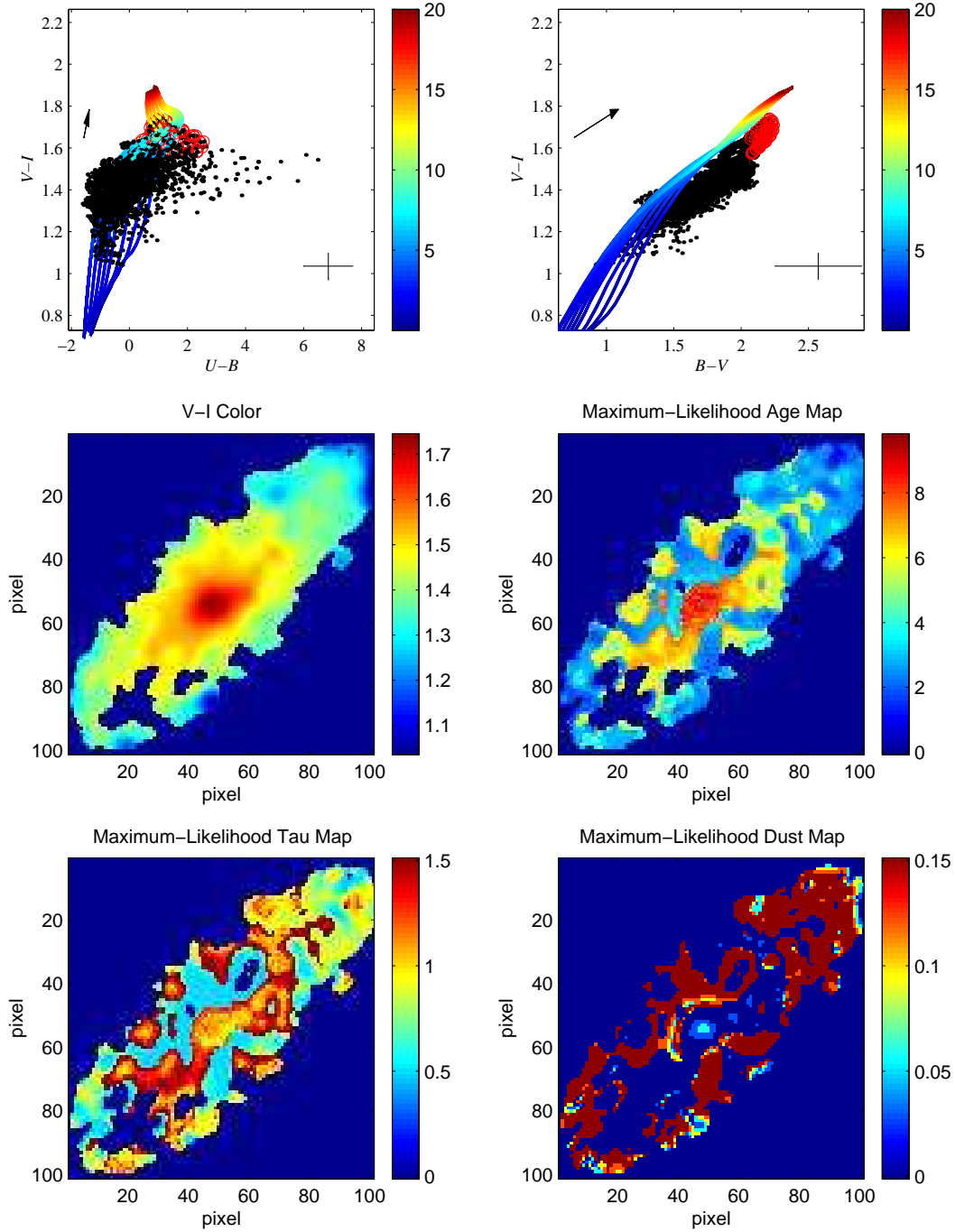
## 3 ILLUSTRATING THE METHOD

Figures 2–4 show results, based upon the colour-colour tracks introduced in §2, for three HDF galaxies subjected to our internal colour-colour analysis. These examples have been taken from the statistically-complete sample given in Table 1 of Bouwens et al (1997), and illustrate the types of conclusions (and their associated uncertainties) we can derive concerning the past star formation history of resolved high-redshift galaxies. We discuss these examples individually here, and defer discussion of the entire sample until §4. Throughout the remainder of this paper objects will be referred to using the identifications given in the Williams et al. (1996) HDF catalogue.

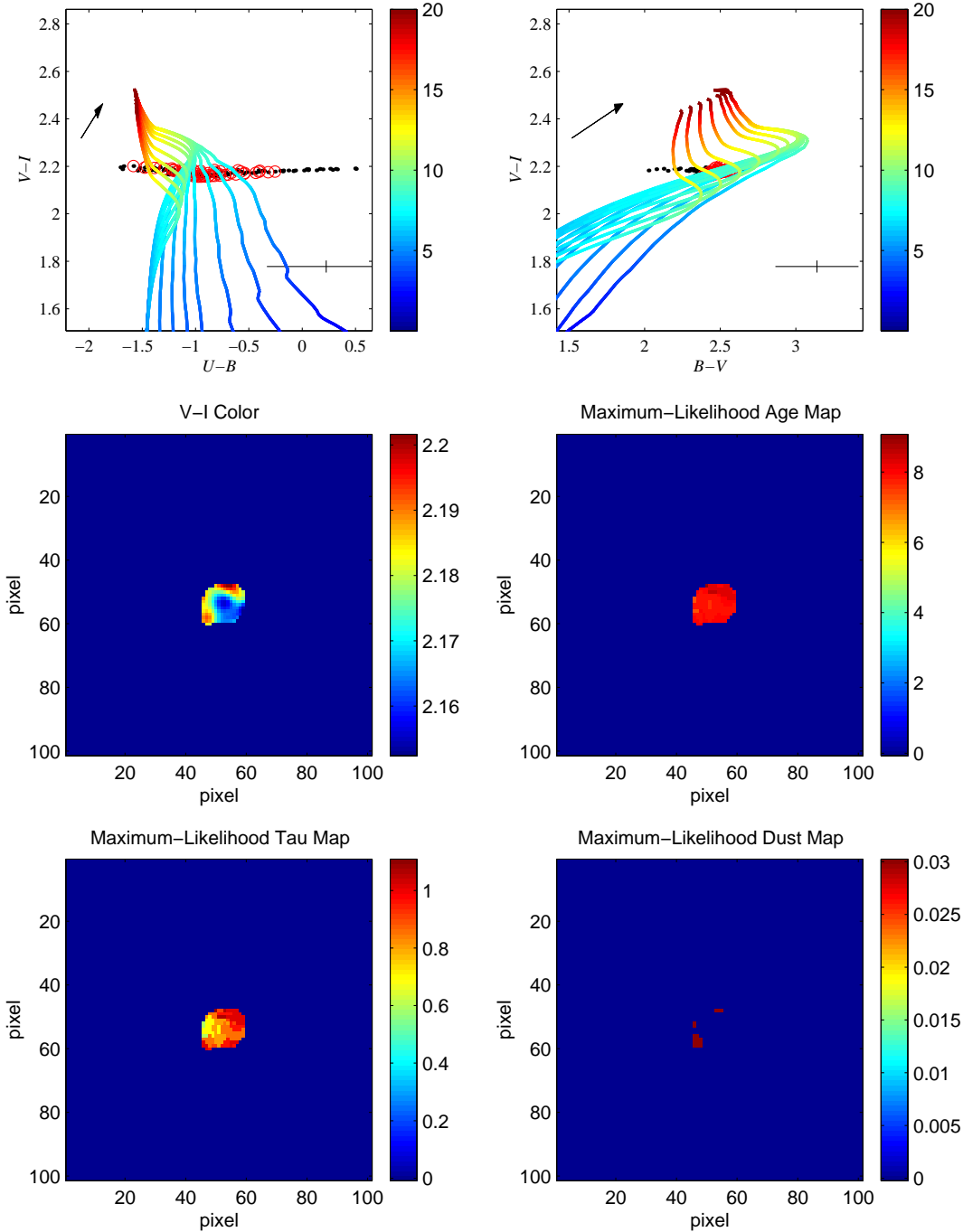
### 3.1 HDF-3.610 – a $z=0.517$ spiral

Figure 2 [middle left] shows the  $V-I$  colour image of a bright ( $I_{814}=19.7$  mag) spiral at  $z=0.517$  in the HDF (HDF-3.610, the third galaxy in Bouwens et al's Table 1). The galaxy has been isolated from the background sky by selecting all contiguous pixels within a surface brightness threshold of  $B_{450}=26.0$  mag arcsec $^{-2}$ . An important consideration in selecting the isophote and the optimum filter is to ensure a minimum signal/noise per pixel over all wavebands. On the one hand, as our eventual sample is  $I$ -selected, it might seem appropriate to select the isophote at a longer wavelength. However, this would bias the pixels selected to those less sensitive to recent star formation and in many cases there would be inadequate signal in the shorter wavelength filters. Were the pixels to be selected according to their  $U$ -band signal/noise, undue preference might be given to strong SF regions particularly for the higher redshift galaxies. We experimented with selection in both the  $B$  and  $V$  bands and found no great difference between the results. In most cases the colour error for each pixel selected according to these criteria is better than 0.2-0.3 mag.

In the top two panels of Figure 2, colour-colour distribution of pixels in the two possible planes ( $V-I$  vs.  $U-B$  and  $V-I$  vs.  $B-V$ ) are compared with the predictions of solar-metallicity, *dust-free* ( $E_{B-V}=0$ ) evolutionary tracks. The tracks shown are purely for illustration – in the full maximum-likelihood analysis the tracks are more finely sampled and dust content is a free variable. Also for illustrative purposes, the colours of pixels in the central region of the



**Figure 2.** Illustration of our colour-colour analysis as applied to a  $z=0.517$  spiral (HDF-3.610) taken from the catalogue of Bouwens et al (1997). Representative dust-free model tracks for solar metallicity are shown in the top two panels, with points corresponding to the colours of individual pixels superposed. Red points refer to pixels within a 5 pixel radius of the center of the image. The pixel-by-pixel colours in the 4 bands are compared to the predictions of the spectral synthesis models for the redshift in question, using a finer model grid than shown in the top panels, and including the effects of variable dust extinction. The spatial colour  $V-I$  map is shown at middle left, and refers to an area  $4 \times 4$  arcsec sampled at the drizzled pixel scale of 0.04 arcsec and limited to contiguous pixels contained within the  $\mu_B=26.0$  mag arcsec $^{-2}$  isophote. The corresponding age, star formation timescale, and dust maps are determined using the maximum-likelihood formulation described in the text. Corresponding best-fit maps for age,  $\tau$ , and  $E_{B-V}$  are shown in other panels.



**Figure 3.** As for previous figure, except showing a coeval, old elliptical system (4.752) at  $z=1.013$ .

galaxy have been coded with red points in the colour-colour plots. For this galaxy the majority of the points lie well within the locus of the  $V-I$  vs  $U-B$  colour space mapped by the tracks, although some red outliers (corresponding to low signal-to-noise points) lie redward of the tracks. On the other hand the majority of points lie slightly systematically redward of the predicted  $V-I$  vs  $B-V$  tracks, suggestive of mild dust extinction. A crucial point is that the *dispersion* in colour-colour space is in excellent agreement with the direction predicted by an age gradient along the colour-

colour tracks. This is a generic feature of the galaxies in the present sample, even amongst those objects that show small systematic offsets from the model tracks (most – but not all – of which can be accounted for by pockets of Calzetti extinction law dust obscuration).<sup>†</sup>

Best fitting age,  $E_{B-V}$  and  $\tau$  maps from the full

<sup>†</sup> Our measure of absolute goodness of fit to a set of model tracks (the mean likelihood over all pixels) will be described in sections 4.1 and 4.2. The example spiral described here has a goodness-

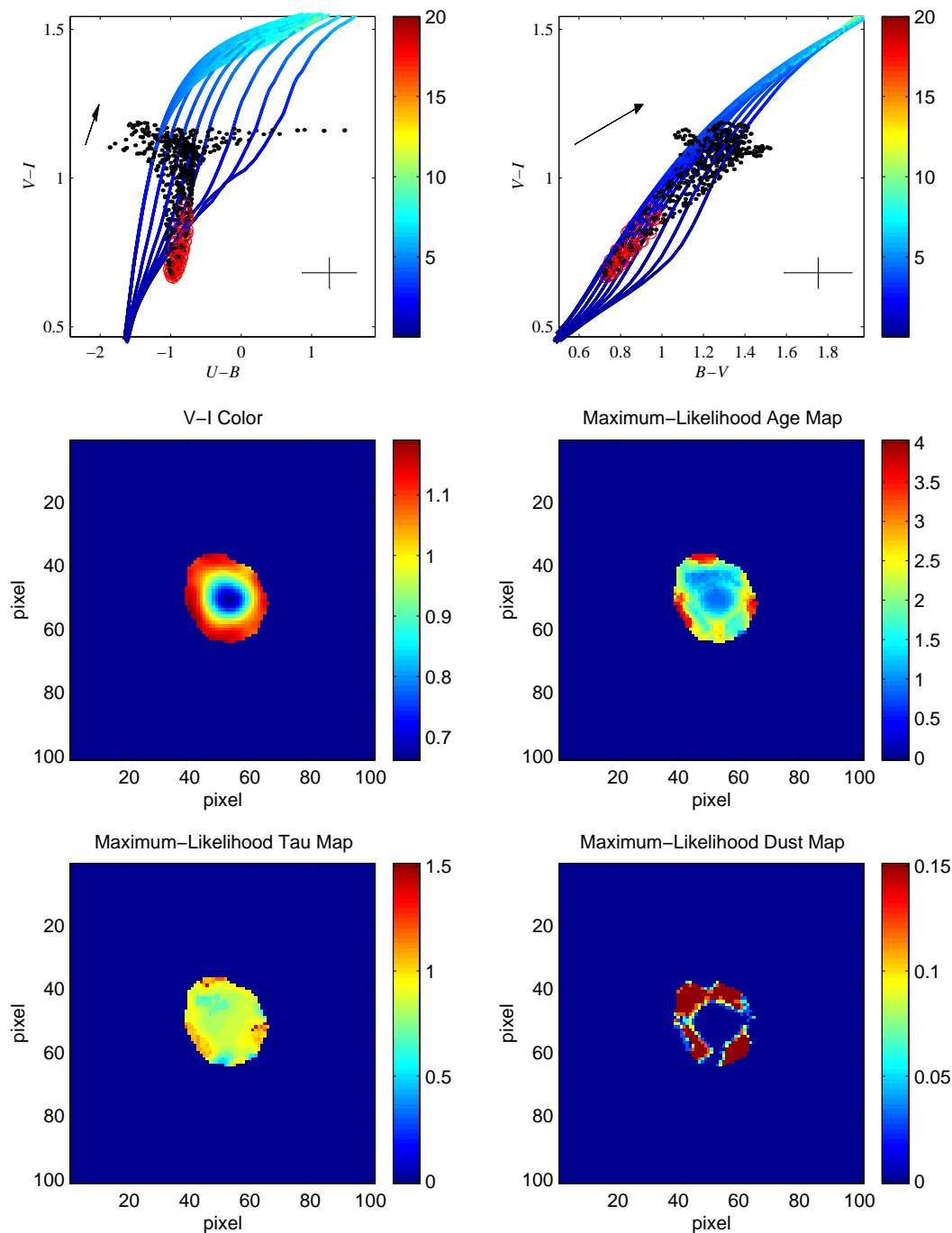


**Figure 4.** As for previous figure, except for an early-type system (HDF-2.264) at  $z = 0.478$  showing evidence of recent star formation.

maximum-likelihood analysis are shown in Figure 2 as separate panels. Parameter ranges are keyed to the vertical colour scale. From an examination of Figure 2 it is clear that this  $z=0.517$  spiral has a bulge which is distinctly redder in all colours and considerably older than that of the disc. More accurately, the optical colours of the disc reflect ongoing star formation in the past 5 Gyr whereas there is

of-fit that is actually slightly worse than the mean for the spiral sample

no evidence that this has been the case for the bulge. It is, of course, not possible to eliminate the possibility that the disc also contains an underlying population of red stars coeval with those of the bulge; its visibility would be difficult to detect given the abundant population of younger stars. Two points emerge from this restriction. Foremost, the relative visibility of the disc and bulge components in the era  $1 < z < 2$  just prior to the epoch of observations, will not be affected. Secondly, the amount of mass involved in

an early population could be constrained from near-infrared luminosities.

As alluded to earlier, significant ( $E_{B-V} \sim 0.1 - 0.15$ ) pockets of patchy dust do improve the fit to the disc colours, but dust is absent from the central regions in this galaxy. In fact the dust seems to be distributed along the inner parts of weak spiral arms, as is often seen in local galaxies. For the comparison shown in Figures 2–4 we have assumed solar metallicity, but as shown in Figure 5 varying metallicity cannot result in synchronization of the ages in the inner and outer parts of this system. The distribution of star formation timescales ( $\tau$ ) shown in Figures 2–4 requires careful explanation. As the tracks in the colour-colour plane show, we have greatest sensitivity to  $\tau$  for populations of intermediate age. For the bulge light there is almost complete degeneracy in solving for  $\tau$ . Accordingly the slight mismatch between the model prediction for  $B - V$  and the observations can swing the fit to a high  $\tau$  whereas the convergence of the tracks at these ages would be compatible with any value. However even for the shortest star-formation timescales the age of the bulge is considerably older than that of the disc, ruling out the possibility that star-formation timescales, rather than age, is responsible for the redder bulge light. In fact no variation in star-formation history, metallicity, or dust alters the basic conclusion that the redder bulge colours are simply due to these pixels originating from the oldest starlight in the galaxy. However Figure 5 does show that varying metallicity within reasonable limits (the excellent agreement between the observed dispersion of colours along the solar metallicity tracks effectively restricts the metallicity of the disc light in this case to  $75\% < Z/Z_{\odot} < 120\%$  Solar) shifts the absolute ages of the various components in this system – confirmation that our technique is best used to study only relative differences in age. In §4 we define a simple statistic which quantifies the relative ages of the inner and outer portions of all spirals in our sample.

### 3.2 HDF-4.752 – a $z=1.013$ elliptical

Our second example (Figure 3) is a high redshift elliptical with  $I_{814}=20.9$  mag. The object is remarkably homogeneous in its  $B - V$  and  $V - I$  colours and consistent with a coeval formation of all visible starlight. The red spectral energy distribution means that the  $U$  image is extremely faint which leads to a large random error in the  $U - B$  colours (except for the brighter central regions coloured red in the colour-colour diagrams shown in Fig. 3). Because the colours of this galaxy correspond (in effect) to a single point on the colour-colour diagram, no particular age-track is mapped out, and thus the system is particularly subject to the well-known age-metallicity degeneracy that plagues analysis of integrated colours of early type systems. This point is shown clearly in Figure 5 (b) which shows the  $V - I$  vs.  $U - B$  colour plane for models with 30% solar, solar and 150% solar metallicities. The key point here is that, although the absolute age inferred is indeed critically dependent on the adopted metallicity, two important conclusions remain unchanged: (i) the light of the galaxy is consistent with a *single* stellar age, (ii) the age is cosmologically significant given the large look-back to this source.

### 3.3 HDF-2.264 – a $z=0.478$ elliptical

The final example (Figure 4) consists of an elliptical with  $I_{814}=21.8$  mag at  $z=0.478$ . In this case there is an obvious spread in the internal colours in this system. We see the same spread in  $U - B$  colours as in Figure 3 corresponding to the lower signal to noise in the  $U$  band for faint sources. However, the nuclear region of the galaxy is significantly bluer than the outer galaxian light, consistent with a younger stellar age (this object might be considered an example of a “blue nucleated galaxy” (Schade et al. 1995), except that it is not morphologically peculiar). This remarkable conclusion holds even when the maximum likelihood analysis attempts to minimize the age spread in this system by invoking a conveniently arranged annulus of dust. The most straightforward interpretation of the colour data is that this E/S0 is *not* a simple stellar system and that some fraction of the starlight was produced within 2 Gyr of the epoch of observation. In the next section we will quantify the frequency of occurrence of cases with such star-formation histories.

## 4 ANALYSIS OF THE BOUWENS ET AL HDF SAMPLE

In order to apply the methodology illustrated above to a representative sample, we now consider the  $I_{814} < 21.9$  mag galaxies in the Bouwens et al (1997) sample, as this constitutes the faintest statistically-complete sample in the HDF with redshift information. Because the model tracks are considerably more degenerate at low redshifts when using the HDF filter set, we will not consider the three galaxies with  $z < 0.3$  in the Bouwens et al list. Thus our sample consists of 28 galaxies with  $0.318 < z < 1.015$ .

Firstly, we consider the distribution of galaxy properties within the broad morphological categories (E/S0: Sabc: Irr/pec/merger) adopted initially by the Medium Deep Survey team (Glazebrook et al 1995). A puzzling feature of the Bouwens et al catalogue is that only a small number (3/31) are apparently ‘Irr/pec/merger’ whereas, within the entire MDS survey to the same magnitude limit, this fraction is close to 30%. In order to check this result and to facilitate comparison with the survey of Brinchmann et al (1997), the Bouwens et al HST images have been reclassified by one of us (RSE) and absolute magnitudes in  $M_{B(AB)}$ , recomputed using K-corrections corresponding to the mean luminosity-weighted age and star-formation history from our model fits. The revised properties of the Bouwens et al sample are listed in Table 1.

We find good agreement between our absolute magnitudes and those of Bouwens et al. However the morphological classifications of a number of systems are rather different. Three objects categorised as spirals by Bouwens et al (HDF-3.400, HDF-3.143, and HDF-4.950, corresponding to #'s 16, 27, 30 in Bouwens’ table 1) have been classed by us as ‘Irr/pec/merger’ and a fourth (HDF-4.402, #22 in Bouwens et al’s table 1) is a marginal case. Although a somewhat subjective correction, the visual classification doubles the number in this category reducing but not eliminating the discrepancy with the MDS counts. However, examination of the Irr number counts within the HDF itself to  $I \simeq 22$  (Abraham et al 1996) does indicate a marginal deficiency

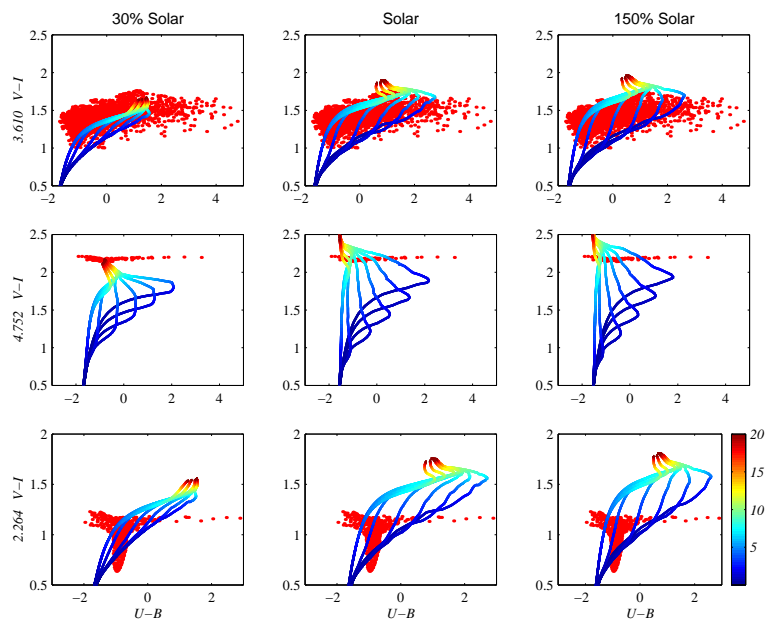


**Figure 5.** The sensitivity of the evolutionary tracks to the adopted metallicity in terms of the  $V-I$  versus  $B-V$  colour plane for the 3 galaxies presented in Figures 2–4. A range in  $\tau$  from 0.1 Gyr to 1.6 Gyr, in steps of 0.2 Gyr, is shown. Columns from left to right correspond to tracks with metallicities of 30% solar, solar, and 150% solar.

**Table 1.** The  $z > 0.3$  Sample from Bouwens et al. (1998). Primary object identifications are correspond to entries in the Williams et al. (1996) catalogue, indexed against entries in Bouwens et al’s table 1. The three galaxies with  $z < 0.3$  are not tabulated.

Williams ID	Bouwens ID	$z$	$m_{I814}$	$M_{B450}$	RSE Class
3.610	3	0.517	19.85	-21.59	S
2.121	4	0.475	20.03	-21.19	Epec
3.386	5	0.474	20.27	-21.25	Spec/Pec
4.656	6	0.454	20.29	-21.10	S
4.744	8	0.764	20.41	-22.39	E
3.350	9	0.642	20.48	-21.81	S
4.795	10	0.432	20.54	-20.65	S
4.241	11	0.318	20.33	-20.21	S0
2.652	12	0.557	20.66	-21.20	Pec
4.550	13	1.012	20.91	-23.03	S
3.534	14	0.319	20.94	-19.58	S
2.251	15	0.960	20.86	-22.92	E
3.400	16	0.473	20.94	-20.64	Pec
3.790	17	0.562	20.93	-20.82	E
3.321	18	0.677	20.92	-21.44	S0
3.264	19	0.475	21.03	-20.37	S
4.752	20	1.013	20.88	-23.37	E
3.659	21	0.299	21.07	-18.99	S
4.402	22	0.555	20.89	-21.06	Spec
4.493	23	0.847	21.17	-22.16	S0
2.514	24	0.752	21.34	-21.44	Sa
3.486	25	0.790	21.46	-21.50	Sp
4.471	26	0.504	21.51	-19.89	E
3.143	27	0.475	21.50	-19.93	Pec
2.264	28	0.478	21.42	-20.15	E/S0
4.402	29	0.556	20.29	-21.60	Pec/Mrg
4.950	30	0.608	21.72	-20.46	Irr
4.928	31	1.015	21.75	-22.30	E

with respect to the more extensive MDS counts which we presume arises simply from small number statistics.

#### 4.1 Spheroidal Galaxies

We begin by addressing the uniformity (or otherwise) and the star formation history of the 12 E/S0 galaxies in the Bouwens et al sample. We note that 2 of the ellipticals (HDF-2.251 and HDF-4.752, #'s 15, 20 in Bouwens et al's table 1) are strong radio sources (Fomalont et al 1997). We discount the first object in Bouwens's table because of its low redshift ( $z=0.089$ ), and also HDF-2.514 which is classed as an elliptical by Bouwens et al. but as an Sa by us.

The key question here, much debated in the recent literature, is whether field ellipticals show evidence of recent star formation, (as expected if they are continuously formed from merging systems (Kauffmann et al 1996) or are coeval in the sense of having formed most of their stars via a single burst at high redshift. The question can be addressed observationally in a number of ways. The only morphological data from HST that has been discussed in this context is that of Schade et al (1998) who illustrate the dangers of relying purely on optical colours to select passively-evolving systems at various redshifts. Their sample of E/S0s from the CFRS/LDSS survey is too small to make strong arguments concerning absolute number densities at various redshifts. However, in terms of surface photometry and colour evolution, their analysis showed that most (morphologically-selected) spheroidals are following the passive evolutionary track albeit with more scatter from galaxy-galaxy than was found for cluster ellipticals (Ellis et al 1997).

Our technique offers a fresh look at this problem since we are able to consider the *internal* homogeneity in the multicolour photometry. Figure 6 shows three representative moderate  $z$  E/S0 galaxies drawn from this sample. It appears that HDF-3.790 and HDF-4.471 are consistent with an old stellar population; our analysis indicates no ongoing SF activity in the 2 Gyr prior to  $z \simeq 0.5$ . The bulk of the SF in such galaxies must have occurred at much earlier times. However, HDF-2.264 shows a much more recent history of SF activity with much of the activity in the previous 0-2 Gyr.

We now wish to examine all of the E/S0 galaxies in this way. Recognising the Bouwens et al sample is obviously small and covers a range in redshift, we seek a simple characterisation of the difference between the two histories discussed above. Foremost it would be helpful to determine whether there is a greater dispersion in the star formation rate of *field* ellipticals compared to their *cluster* counterparts. Rather than interpret the data in the context of hierarchical models (Baugh et al 1996, Kauffmann 1996) we first seek an empirical comparison between two such samples.

For each spheroidal galaxy in the Bouwens sample, our methodology enables us to measure the fraction of the stars formed in the last third of the galaxies' lifetime,  $\Psi_{1/3}$ , where we define the start of the galaxy's lifetime as the age of the oldest pixel in the image. This is given for various metallicities and dust assumptions in Table 2.

$\Psi_{1/3}$  is a useful physical measure for several reasons. Most importantly, as Table 2 shows, it is fairly robust to changes in the assumed metallicity. Whereas absolute ages depend crucially on metallicity, the *relative* ages of young

and old stellar populations are largely unaffected. It is also a quantity that can readily be predicted in those hierarchical models which assume E/S0 galaxies are continuously produced via merging of gaseous dark matter halos (Kauffmann et al 1996). In the case where ellipticals form by monolithic collapse at high redshift ( $z_F > 3$ ) one expects  $\Psi_{1/3} \simeq 0$  for all objects. The critical question then is the extent to which non-zero values in Table 2 are informative and, in particular, differ from what is known about cluster ellipticals at high redshift.

Resolved multi-colour data of comparable quality does not exist for any sample of distant cluster ellipticals. Given some assumptions, the tight photometric scatter in the rest-frame ultraviolet colours of cluster ellipticals (Ellis et al 1997, Stanford et al 1998) can be used to derive upper limits to recent star formation in those galaxies. In what follows, we examine a preliminary comparison of cluster and field star formation histories.

Following Bower et al (1992), we assume that the scatter in rest-frame  $U - V$  colour originates in secondary bursts of star formation in the last few Gyr prior to the epoch of observation. For the cluster ellipticals analysed by Ellis et al, whose mean redshift is  $\langle z \rangle = 0.55$ , the observed rms scatter for the E/S0 population is  $\delta(U - V) = 0.06$  mag  $\pm 0.01$ . If this scatter is produced by secondary episodes of star formation, we can estimate the value of  $\Psi_{1/3}$  consistent with the observed scatter. Applying this to the ellipticals in Coma and Virgo for which the observed scatter is  $\delta(U - V) = 0.04$  mag, Bower et al concluded that, at most, 10% of the stellar mass could have been created in secondary bursts in the previous 5 Gyr, i.e.  $\Psi_{1/2} < 0.1$ . In a more recent analysis however Bower et al (1998) concluded that such constraints are rather weak when applied locally particularly in truncated star formation histories.

Noting these uncertainties will be reduced at larger look back times where we are closer to the initial burst, a direct application of the same methodology for the Ellis et al  $z=0.55$  cluster sample yields  $\Psi_{1/3} < 0.08$  rms for the cluster population. As a working definition, therefore, we will therefore assume that  $\Psi_{1/3} < 0.05$  corresponds to a single-burst elliptical which formed all its stars at a formation redshift  $z = z_F$ . Given the mean redshift of our E/S0 sample is  $\bar{z} \simeq 0.7$ , in an Einstein-de Sitter universe with  $H_0 = 70$  kms  $s^{-1}$  Mpc $^{-1}$ , this constraint essentially implies a constant comoving density of ellipticals to  $z \simeq 1.5$  for  $z_F \simeq 3$ . For  $\Omega = 0.05$ , the constraint is only slightly weaker ( $z \simeq 1.3$ ). In the monolithic collapse model, we would not expect any of our field ellipticals to have  $\Psi_{1/3} > 0.05$ .

Examining Table 2, we can see that 4/11 of the faint E/S0s in the sample show signs of recent star-formation according to the above definitions. This implies the majority, though not all, of the field E/S0s in the HDF completed the bulk (95%) of their star formation before  $z \simeq 1-1.5$ . There is no obvious trend with the galaxies which show evidence for recent star formation. HDF-2.251 is in this category and is a strong radio source, but so is HDF-4.752 which has a low  $\Psi_{1/3}$ . Where we believe the ellipticals can be distinguished from the S0s, there is no correlation with  $\Psi_{1/3}$ .

It seems most unlikely that those few spheroidals which show a colour dispersion could be explained as old systems with metallicity gradients. As Figure 1 shows, even extreme metallicity variations would be insufficient to account for

**Table 2.** Early Type Galaxies: Fractional Star-formation in Last 1/3 of Lifetime

ID	$z$	solar + dust			30% solar + dust			solar + no dust			comment
		$\Psi_{1/3}$	$\langle \mathcal{L} \rangle^a$	$\langle E_{B-V} \rangle^b$	$\Psi_{1/3}$	$\langle \mathcal{L} \rangle$	$\langle E_{B-V} \rangle$	$\Psi_{1/3}$	$\langle \mathcal{L} \rangle$	$\langle E_{B-V} \rangle$	
2.121	0.475	0.012	0.601	0.020	0.000	0.678	0.027	0.006	0.596	0.000	E (coeval)
4.744	0.764	0.002	0.584	0.001	0.000	0.822	0.009	0.001	0.583	0.000	E (coeval)
4.241	0.318	0.230	0.743	0.017	0.212	0.650	0.021	0.208	0.739	0.000	S0
2.251	0.960	0.092	0.791	0.098	0.053	0.777	0.061	0.059	0.709	0.000	E
3.790	0.562	0.019	0.312	0.003	0.002	0.611	0.004	0.016	0.312	0.000	E (coeval)
3.321	0.677	0.003	0.597	0.006	0.000	0.842	0.029	0.002	0.592	0.000	S0 (coeval)
4.752	1.013	0.004	0.920	0.003	0.000	0.748	0.007	0.006	0.918	0.000	E (coeval)
4.493	0.847	0.001	0.885	0.022	0.000	0.827	0.039	0.001	0.858	0.000	S0 (coeval)
4.471	0.504	0.005	0.400	0.000	0.001	0.583	0.013	0.005	0.400	0.000	E (coeval)
2.264	0.478	0.365	0.807	0.070	0.278	0.733	0.047	0.318	0.757	0.000	E/S0
4.928	1.015	0.058	0.350	0.144	0.036	0.709	0.121	0.040	0.192	0.000	E

<sup>a</sup> Mean likelihood for all pixels.

<sup>b</sup> Mean rest-frame relative  $B - V$  dust reddening for all pixels.

the colour variations, and in any case such variations would have to operate in the direction of *depleting* the core of the elliptical, which is opposite to local observations which find the cores of ellipticals to be relatively enriched.

The robustness of this result, which suffers of course from the small sample size in the tiny field of the HDF, can be considered by examining  $\langle \mathcal{L} \rangle$ , the mean likelihood for all the pixels in the fit. Tests indicate a value above 0.6 is a reasonably good fit to the colour distribution. Table 2 also lists  $\langle E_{B-V} \rangle$ , the mean  $E_{B-V}$  reddening in the rest frame across all the pixels. Even allowing dust to be a free parameter, the only elliptical which shows any evidence for appreciable dust signature is the most distant example, HDF-4.928.

Does the large fraction (7/11) of galaxies with  $\Psi_{1/3} < 0.05$  contradict the claim (Kauffmann et al 1996) that by a redshift of 1, the comoving volume density of passively evolving red ellipticals should have declined by a factor of 3? A detailed comparison must await more data but it is interesting to consider the matter briefly notwithstanding the uncertainties. Semi-analytical models do predict a substantial amount of merging at late times. A preliminary inspection of the merging histories of massive field ellipticals at  $z \simeq 0.7$  suggests somewhat higher percentages of star formation in the previous few Gyr than indicated in Table 2 (Cole, private communication).

At face value therefore, there appears to be limited evidence for a more diverse star formation history for HDF field ellipticals compared to their rich cluster counterparts at similar redshift and, to the extent that comparisons with hierarchical models can be currently made, the scatter seems somewhat less than predicted. However, an important point to recognise in these comparisons is the different techniques used in the field and cluster data and, more fundamentally, what is meant by an ‘elliptical’ in the numerical simulations. For example, a centrally-concentrated but asymmetric galaxy with tidal tails would probably not be classified by an observer as an early-type system, while such a system might be classed as an elliptical in a semi-analytical model on the basis of bulge-to-disk ratio.

It is also worth emphasising that our analysis is really addressing the history of ellipticals only from one partic-

ular viewpoint. Rather than measuring the absolute number density of systems that remain passively red at various redshifts (c.f. Kauffmann et al 1996), we are here examining the history of recognisable *spheroidal products*. It seems, from the number counts in the HDF that these represent a substantial fraction of the present day population of E/S0s. What we find is that only a few of these show evidence of recent mergers through signatures of star formation. Of course this may be simply because to produce a smooth product recognisable by us as a E/S0, the merger *had*, by definition, to have occurred at an epoch such that  $\Psi_{1/3} < 0.05$ . The ultimate resolution of this problem would then lie in the joint luminosity-colour distribution of a large sample of morphologically-selected field spheroidals (Menanteau et al, in preparation).

## 4.2 Disc and Bulge Histories

We now turn to discuss the sample of 13 spirals from Table 1. As noted earlier, our classifications are in reasonably good agreement with those of Bouwens et al. *except* for a number of systems that Bouwens et al. classify as spirals which we class as morphologically peculiar. In order to ensure that at least no intermediate-late spirals are missed in our analysis, and recognizing that classification of morphological peculiarities is rather subjective, Table 3 includes *all* objects classified by Bouwens et al. as spirals, including several galaxies which we class as peculiar or merging. As usual, we excluded systems whose redshifts were below  $z = 0.3$ . For reference, our own morphological classifications are shown as the final column in Table 3.

In the case of the spiral galaxies we are interested in addressing a number of questions. The first issue (hitherto unaddressed in HST studies) relates to the relative ages of bulge and disc components. Figure 7 indicates the relative star formation histories for light inside and outside a five pixel radius aperture centred on each of three spiral galaxies in our sample. In this paper no attempt has been made to do a photometric decomposition on these images, but throughout the remainder of this paper we will refer to the the light interior to the aperture as the ‘bulge’, and exterior

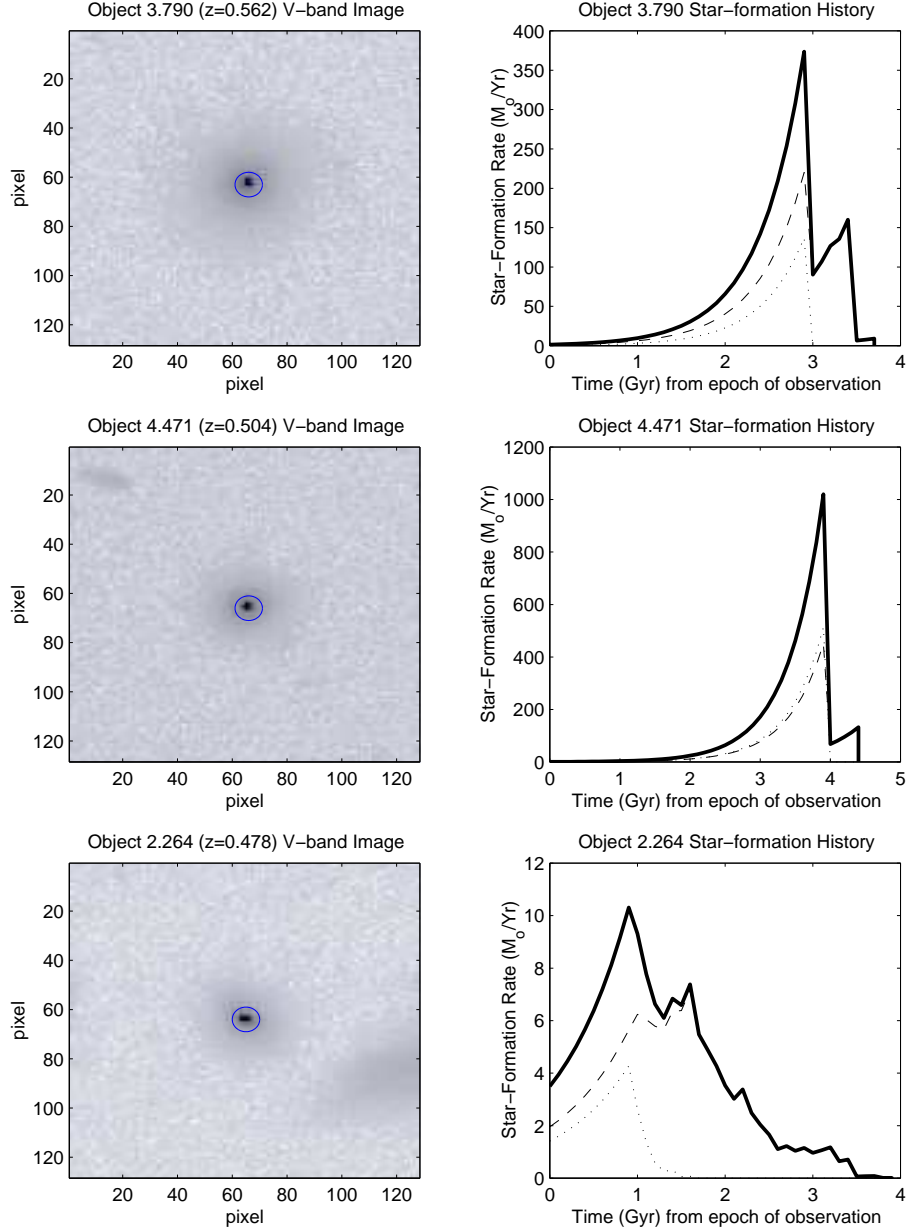


**Figure 6.** *V*-band images (left) and star formation histories (right) for 3 spheroidal galaxies from the sample of 12 E/S0s from Bouwens et al’s list. The dotted curve on the right refers to the history for pixels within the five pixel inner aperture shown on the left, corresponding to the nuclear light. The dashed curve refers to the light exterior to this aperture, and the solid curve refers to the entire galaxy. Models assume solar metallicity and no reddening.

to the aperture as the ‘disc’, both for convenience and because the 5 pixel radius was chosen so that bulge light clearly dominates the interior of the aperture for all galaxies with an obvious bulge in the I-band images. It is clear that the inner and outer parts of the galaxies in Figure 7 have undergone remarkably different star-formation histories. The ratio of the *median* ages of the bulge and disc light,  $T_{B/D}$ , is given in Table 3 for various dust and metallicity assumptions. We have included irregular and peculiar systems in this tabulation, as well as spirals. As with the earlier statistic used to quantify the star-formation history of ellipticals, the  $T_{B/D}$  statistic, which is a measure of *relative* age, is remarkably robust to changes in metallicity and dust con-

tent. In the case of the 3 illustrated spirals, a mean ratio of 1.54 emerges indicating the bulges (more accurately, the inner parts of the galaxies) are 50% older than the outer parts with little recent activity. This ratio is somewhat larger than the mean for the entire sample, but the general result that clearly emerges is that median age of bulges is substantially older than the median ages of discs. In Table 3 we delineate systems as having an ‘old bulge’ if  $T_{B/D} > 1.1$  for *all three* model scenarios, ie. requiring the inner light to be 10% older than the outer light regardless of assumptions made with regard to metallicity or dust content. Six of the nine morphologically normal spirals pass this very stringent test. A further two have  $T_{B/D} > 1$  for all three models, but with

the relative age difference below 10%. Only a single spiral has  $T_{B/D} < 1$  for *any* choice of metallicity or dust fraction, and even in that case the bulge is only younger than the disk for one of the three model scenarios, and at a negligible level (0.5%). The result that clearly emerges from our investigation is that, for morphologically normal systems, *bulges are indeed always the oldest parts of galaxies*. This remains true even in the face of possible metallicity gradients, which are not modelled in this paper. Based on observations in our own Galaxy and in the Local Group, the general expectation is of course that bulges would have generally lower metallicity than disks. This results in relatively *older* bulges, since generally speaking decreasing metallicity results in increased age at a given colour, as shown in Figure 1. As emphasized earlier, Table 3 shows this is an extremely robust result that is independent of assumptions made with regard to metallicity and dust.

We note that the bulges in the morphologically normal spirals considered here, even in the oldest cases, do not appear to be as uniformly red and old as the oldest ellipticals discussed in §4.1. This may be partly the result of photometric contamination by underlying disk light (although the rather small 5 pixel radius aperture was chosen to minimize these effects), but it must also be remembered that the mean look-back to the latter sample is 1-2 Gyr higher.

For the four morphologically peculiar systems in Table 1, a rather different picture emerges. Only one of these passes our stringent ‘old bulge’ test, with two of the remainder showing quite clear evidence for a systematically younger bulge. The star-formation histories of morphologically peculiar galaxies, including these systems (which are clear examples of the “Blue Nucleated Galaxies” reported in Schade et al. 1995), will be considered in detail in a subsequent paper

The second substantial issue we wish to address with our analysis of morphologically normal spirals, following the studies of Brinchmann et al (1997) and Lilly et al (1997), is the suggestion from these papers that large disc galaxies are well-established systems with a declining star formation history. Brinchmann et al found the redshift distribution,  $N(z)$ , of the CFRS/LDSS spirals was more extended than would be expected in a no-evolution case. Very approximately, they concluded 1 mag of luminosity evolution would be needed by  $z \simeq 1$  to reconcile predictions with the data. Lilly et al (1997) analysed the surface photometry of the larger spirals and found a similar effect. Specifically, over  $z < 0.7$  they found a surface brightness evolution of  $\Delta\mu_B = -0.8$  mag. The trends are somewhat stronger than those found in the dynamical study of Vogt et al (1997) although differences in the way in which galaxies are selected can crucially affect the interpretation, as Lilly et al discuss.

For the examples shown in Figure 7, our analysis indicates a strongly-declining total star-formation rate with time and suggests a peak activity 1-3 Gyr earlier. Over the entire sample this is a fairly consistent trend. The mean redshift of the sample is  $\bar{z} = 0.55$ , somewhat lower than for the E/S0s, and thus the peak activity for the population would, in most cases, occur at  $z \simeq 1$ .

The bulk of the luminosity evolution inferred in the spiral population clearly arises from the fading discs. We can therefore ask whether the trends seen for the large face-on spirals in Figure 7 are consistent with the evolution in

blue light inferred from the CFRS/LDSS sample. To examine this we took the luminosity-weighted timescale  $\tau$  (c.f. §2.1) and mean age for representative galaxies and estimated their rest-frame evolution in  $M_B$ . As expected, the results depend much more sensitively on the input assumptions but, in general, the results imply  $\simeq 0.5$  mag over  $0.5 < z < 1$  which is consistent with the CFRS/LDSS constraints.

### 4.3 Global Histories

The detailed analysis of the colour distribution of individual galaxies and those of a given morphology has given a good indication of the advantages and restrictions of our method. However, if we wish to ultimately derive conclusions concerning the star formation history of volume-averaged populations, we need to extend the techniques taking into account the detectability of each galaxy as a function of  $z$  and the relative masses involved in the various star formation phases. This is an important point notwithstanding the conclusions in §4.1-4.2 since, as various authors have discussed (White 1996, Brinchmann et al 1997) morphology may be a transient property. In principle our method offers an opportunity to examine more general trends – as discussed in the next section. A major conceptual advantage of our method is that by focussing on star-formation history on a pixel-by-pixel basis, we probe galaxian star-formation history in a manner that is meaningful even in the face of morphological transformations. Even in an evolutionary scenario dominated by density evolution, stars from the merger fragments are still present in the merger product. So the structure of the star-formation history curves shown in Figure 7 is a partial record of the formation history of the stars in the final system, even if we have no information about the morphologies of the fragments. We can thus consider whether the Bouwens et al galaxy sample is predominantly the result of star-formation activity which peaked at  $z \simeq 1-2$ , as claimed by Madau et al 1998.

There are several complications in conducting such calculations. Firstly, taking this approach requires us to assume *absolute* ages for the galaxy sample, rather than the more robust relative ages for internal galaxian components, upon which we have focussed so far. An equally important complication is that the Bouwens et al sample is flux-limited and so spans a range in look-back time and luminosities. To convert discrete realisations of the SF history  $\Psi_i(t)$  for  $i=1, N$  objects spanning a range of redshifts  $z_i$ , into its comoving average,  $\Psi_T$ , we must adopt a cosmological model  $t(z, H_o, \Omega)$ , and weight each  $i$ th contribution by  $1/V_{max}$  (Schmidt 1968; Bouwens et al. 1998):

$$\Psi_T(z) = \sum_{i=1}^N 1/V_{max} \Psi_i[z_i, z(t, H_o, \Omega)] \quad (3)$$

As an illustration of this, we have attempted to combine the histories  $\Psi_i(t)$  for most of the galaxies in Table 1 in order to produce an estimate of the global history  $\Psi_T(z)$  (Figure 8) where we compare our results with that of Madau et al (1997). We show curves as an envelope whose limits correspond to 30% solar and 150% solar metallicity for the entire sample. We cut off the diagram at  $z = 1.5$  (with the last observational data point corresponding to  $z = 1.2$  because of the small sample size considered – at  $z \sim 1.5$  one or two individual bright galaxies dominate the total star-formation history plot, and Poisson errors become domi-

**Table 3.** Spiral Galaxies: Ratio of Inner to Outer Median Age

ID	$z$	solar + dust			30% solar + dust			solar + no dust			comment
		$T_{B/D}$	$\langle \mathcal{L} \rangle^a$	$\langle E_{B-V} \rangle^b$	$T_{B/D}$	$\langle \mathcal{L} \rangle$	$\langle E_{B-V} \rangle$	$T_{B/D}$	$\langle \mathcal{L} \rangle$	$\langle E_{B-V} \rangle$	
3.610	0.517	1.490	0.829	0.084	1.212	0.884	0.105	1.783	0.804	0.000	Spiral – old bulge
4.656	0.454	1.400	0.919	0.063	1.214	0.791	0.027	1.154	0.838	0.000	Spiral – old bulge
3.350	0.642	1.231	0.947	0.094	1.316	0.925	0.047	1.200	0.866	0.000	Spiral – old bulge
4.795	0.432	1.294	0.844	0.040	1.727	0.691	0.016	1.421	0.816	0.000	Spiral – old bulge
4.550	1.012	1.222	0.915	0.065	1.185	0.863	0.077	1.290	0.882	0.000	Spiral – old bulge
3.534	0.319	1.571	0.926	0.031	1.667	0.860	0.025	1.471	0.838	0.000	Barred Spiral – old bulge
3.400	0.473	1.000	0.904	0.056	0.625	0.867	0.051	0.875	0.865	0.000	Peculiar
3.264	0.475	1.308	0.902	0.103	1.261	0.924	0.080	1.095	0.769	0.000	Spiral
3.659	0.299	1.115	0.705	0.048	1.167	0.696	0.044	1.067	0.685	0.000	Sab
4.402	0.555	0.400	0.762	0.039	0.500	0.682	0.030	0.500	0.728	0.000	Spec
3.486	0.790	1.643	0.899	0.085	1.833	0.857	0.071	1.400	0.865	0.000	Spiral – old bulge
3.143	0.475	1.467	0.945	0.050	1.250	0.831	0.012	1.250	0.900	0.000	Peculiar – old bulge
4.950	0.608	1.000	0.873	0.013	1.000	0.739	0.002	1.167	0.857	0.000	Irregular

<sup>a</sup> Mean likelihood for all pixels.

<sup>b</sup> Mean rest-frame relative  $B - V$  dust reddening for all pixels.

nant. The curves correspond to the volume-averaged star-formation histories for all spirals, peculiars, irregulars, and the four “young” ellipticals in the sample. “Coeval” ellipticals have been excluded from consideration because the contribution at high redshift from these systems depends crucially on their adopted absolute ages (which are very poorly constrained because, by definition, they have little dispersion in internal colour). In any case these systems are likely to contribute mostly at  $z > 1.2$ .

Although clearly an approximation (whose correctness is subject to the necessity for assuming absolute, rather than relative, ages in the calculation), the extrapolated star-formation history of the Universe calculated by adding together results from just  $\sim 20$  galaxies in the Bouwens sample approximates that obtained completely independently from deep galaxy surveys. At redshifts  $z > 0.5$  the survey data points lie slightly below the predicted curve from our analysis, but this may not be significant given the rather large uncertainties on both the models and the data points, and given the omission of “old ellipticals” (which must be contributing a small amount of star formation even at  $z < 1.2$ ) from the models.

At face value Figure 8 suggests that roughly all the starlight located in deep surveys at  $z < 1.2$  ultimately ends up in galaxies represented by the systems in the Bouwens sample. While interesting, this conclusion is highly uncertain, not least because of the very small sample size used in this extrapolation. In particular, we have already noted there is an apparent deficiency of irregular/peculiar/merger galaxies in the Bouwens et al sample compared to wider field HST studies. If the  $z < 1$  inventory is richer in star forming systems whose evolution is important (as suggested by the results of Brinchmann et al) then either the contribution of late type systems beyond  $z \simeq 1$  cannot be dominant or the extrapolation is unreliable. An obvious example would be the presence of dust, not in the currently-observed Bouwens et al sample or additional sources thought to be under-represented at  $z < 1$ , but perhaps in their predecessors seen at earlier times. At this stage, this is largely speculation. The

major result is the predictive power of our colour-based techniques particularly when enhanced with larger and deeper samples.

## 5 DISCUSSION

It is interesting to contrast our method with the approach of Brinchmann et al (1998) who derived luminosity functions and volume-averaged luminosity densities for morphological subsets from the combination of HST imaging and ground-based redshift surveys for  $\simeq 300$  field galaxies. Whilst they discussed the validity of the assumption that the morphological type is a time invariant property, their analysis was primarily concerned with calculating the contribution of each class to the redshift-dependent star formation rate. They found the greatest rate change with redshift over  $0 < z < 1$  belonged to galaxies of irregular morphologies although the largest contribution to the volume-averaged total at  $z \simeq 1$  was from disc galaxies. Brinchmann et al argued that it is unlikely that the rapidly declining population of galaxies with irregular morphologies transform to form large disc galaxies given the contrast in evolutionary trends.

Even with  $> 300$  galaxies with redshifts and HST morphologies, once the sample is broken into redshift and morphology bins, the statistics necessary to reach convincing conclusions becomes marginal. Furthermore, the likelihood of a possible migration from one class to another as the star formation rate changes or, more simply, a fading below the detection limit as the rate declines could easily complicate the above conclusions.

Our technique offers a number of ways with which to overcome the limitations of the Brinchmann et al analysis. Foremost, we can address in more detail the question of the homogeneity in the star-formation history of a given class. The issue here is not simply the scatter from one galaxy to another within a given class, but the dispersion in internal pixel colours and the implications of this for the star-formation histories. Admittedly there is no short cut to having a fair and representative sample of galaxies to

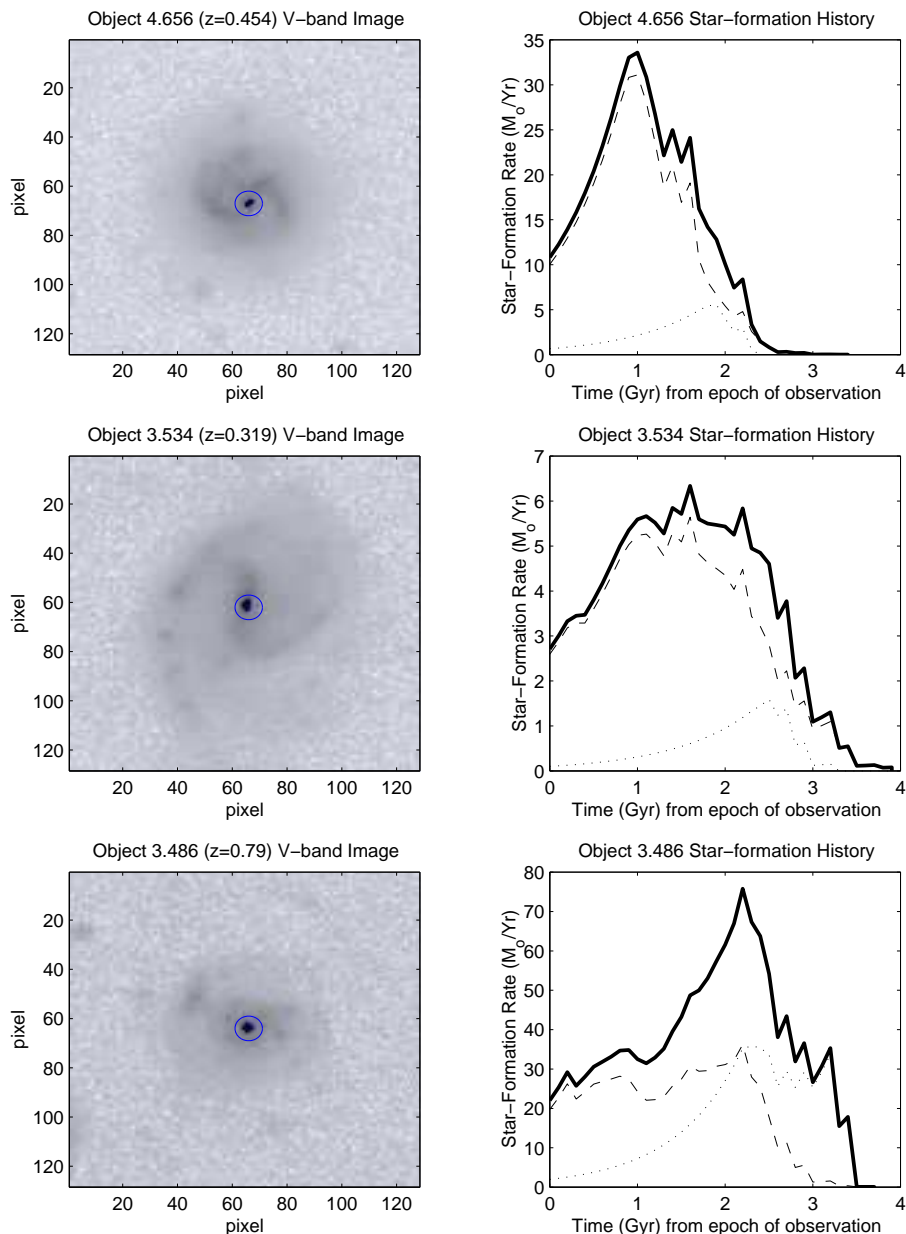


**Figure 7.** As for Figure 6, for a sample of spirals from the Bouwens et al sample. The dotted curve corresponds to the aperture shown on the left, which isolates bulge light. The dashed curve corresponds to pixels outside this aperture, and the solid curve is the history for the entire galaxy.

analyse, but the availability of resolved data opens up a much more powerful tool for addressing issues related, for example, to the question of whether most field ellipticals are simple coeval stellar populations. The second advantage of our method is that we can, within the limitations discussed earlier, by focussing on star-formation sidestep the difficulty of not knowing the precursor population of each class. Indeed, in principle, we can abandon morphological categories altogether and simply isolate those  $z < 1$  galaxies which are likely to have dominated the star formation history 2-5 Gyr earlier. Finally, of course, we can address the history of distinct sub-components such as bulges and discs.

It is important to consider ways to verify the validity of many of our conclusions. Concerning the issue of whether

spheroidal galaxies are being continuously produced, our approach in examining evidence in the colours for recent mergers can be easily extended to higher redshifts. The technique complements other approaches based on colour distributions. For the disc galaxy evolution, it will be possible to verify our star formation rates directly, and constrain dust content, once integral field spectroscopy becomes feasible to the necessary surface brightness limits. The greatest restriction in the application of our method is the need for redshifts which, presently, restricts the HDF sample to only 32 galaxies. By extending the HDF surveys to deeper spectroscopic limits or perhaps adopting photometric redshifts, this restriction can be partially overcome. A greater redshift range would allow intermediate redshift samples to be

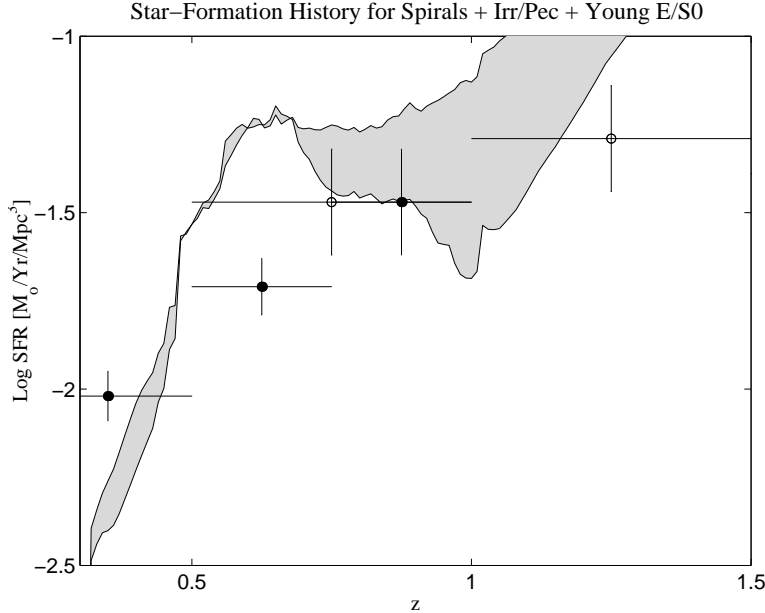


**Figure 8.** The global star-formation history of the universe obtained by adding the contribution from the spirals, irregulars and evolving ellipticals in our sample. The recovered total star-formation history assuming 30% solar metallicity for all galaxies is shown as the top curve, with the corresponding curve for 150% solar metallicity shown as the bottom curve. The interior region (shaded gray) thus corresponds to the region of the diagram possible for a mixture of metallicities. Calzetti-law dust extinction was assumed for all curves. The solid points correspond to data from the CFRS survey (Lilly et al 1996), as given in Madau et al. (1996). Open circles correspond to estimates based on photometric redshifts in the Hubble Deep Field (Connolly et al 1997).

directly compared with their statistical ancestors for consistency purposes.

A second enhancement is the extension of our method to near-infrared passbands. Without infrared observations to help constrain the appropriate dust law, it is difficult to constrain definitively the possible interplay between dust and genuine stellar histories. Even with ground-based photometry, the integrated near-infrared magnitudes offer a way to verify the global properties inferred for a given galaxy, but ultimately we can expect to use NICMOS data to extend the full resolved colour-colour analysis. Later papers in the series will take these ideas forward and address more closely the role of the star forming irregulars thought to be dominant in the intermediate redshift range.

## 6 CONCLUSIONS

We summarise our conclusions as follows:

1. The spectral synthesis modelling of the spatially resolved internal colours of galaxies of known redshift is an important new technique for probing galaxy evolution, offering a number of benefits compared to studies based on integrated colour alone. The technique makes an explicit connection between evolutionary history and stellar populations. We use the dispersion around colour-colour tracks to distinguish between models that are degenerate in terms of integrated colour enabling the dust content to be explicitly parameterized and allowing the star-formation histories of physically-distinct galactic subcomponents to be recon-

structed. Most importantly, internal colour analyses enable robust studies of *relative ages* addressing the homogeneity of stellar populations and probing the order in which galactic components have been assembled.

2. Most early-type systems (7/11) in the Bouwens et al. redshift sample have internal colour dispersions consistent with being old and coeval, but (adopting  $\Psi_{1/3} < 0.05$  as the criterion for an old, coeval system) *over one-third [4/11] of the early type systems studied do not*. This result contrasts with that derived from the scatter in colour-magnitude diagrams for populations of spheroidals in distant rich clusters. The field sample is much too small for detailed conclusions to be drawn regarding the star-formation history of early type systems as a class, but the current fraction ( $\sim 40\%$ ) of young early-type systems is reasonably consistent with the predictions from hierarchical models. If one adopts a less stringent definition for old, coeval system (say  $\Psi_{1/3} < 0.1$ ) then the constraints on hierarchical models become substantially tighter. We therefore suggest that specific predictions for the distribution of  $\Psi_{1/3}$  would provide a valuable test of the success of hierarchical models. However, quantifying the fraction of young early-type galaxies expected in such scenarios depends on how quickly such systems relax after a merger event, and hence how such systems are classified both visually and on the basis of n-body/semi-analytic models. Similar criteria must be adopted for both observations and models.

3. We find that the bulges in the HDF spirals are generally redder than their disks with a median age unambiguously older in the majority (6/9) and at least as old as the disk in most of the remainder (2/9). Bulges exhibit qualitatively different star-formation histories from their surround-

ing disks indicating a short initial period of star-formation followed by relative quiescence. Unless bulges are heavily enriched relative to disks, these results strongly support the “traditional” picture for the formation of bulges and pose a serious challenge to competing secular evolution models.

4. The overall dust content in galaxies from the Bouwens et al sample at intermediate redshifts  $0.3 < z < 1.0$  is fairly similar to that seen locally. Spirals and irregulars exhibit evidence for patchy pockets of dust at the  $E_{B-V} \sim 0.1$  level, but the majority (10/11) of early-type galaxies appear essentially dust-free. No galaxy in this sample appears to have internal colour dispersions suggestive of major obscuration nor internal colours dominated by dust as opposed to age or star-formation history. As in the local Universe, dust in the intermediate-redshift Universe ( $z < 1$ ) appears to play a subsidiary role in the interpretation of galaxy morphology and number counts. Our conclusions are dependent, however, on the universal validity of the Calzetti (1997) extinction law and independent tests of the applicability of this law over a range of redshifts and galaxy types are of the first importance.

5. The star-formation histories we infer for field spirals agree with those derived from deep galaxy surveys. If significant morphological transformations have not occurred within our spiral sample, then our declining star-formation histories are consistent with typical fading in disk light by  $M_B \sim 0.4$  mag between  $z = 1$  and  $z = 0.5$ , in agreement with the values obtained from the CFRS and LDSS surveys (Brinchmann et al. 1998; Lilly et al. 1998). The peak in the volume-averaged star-formation activity contributed by starlight in  $z \sim 0.5$  disc galaxies occurred close to  $z = 1$ .

6. As our methodology focusses on the stellar content (rather than on the bulk morphological properties), we illustrate how an approximate inventory of the total starlight in our galaxy sample can be backtracked towards the formation epoch without assuming that morphologies are preserved. Surprisingly, we recover the bulk of the starlight seen in deeper surveys. The present sample is very small and this is a tentative result, particularly as there is some evidence that the Bouwens et al sample is deficient in star forming galaxies. However, if confirmed, it would suggest that star-formation at  $z < 1.2$  is not occurring dominantly in systems which have escaped detection in deep optical surveys.

#### Acknowledgments

We thank Simon Lilly, Simon White, Sidney van den Bergh, Max Pettini, Jarle Brinchmann, Rychard Bouwens, and Felipe Menanteau for useful discussions and suggestions.

#### REFERENCES

Abraham, R. G., Tanvir, N. R., Santiago, B. X., Ellis, R. S., Glazebrook, K., van den Bergh, S. 1996a, MNRAS, 279, L47  
 Abraham, R. G., van den Bergh, S., Ellis, R. S., Glazebrook, K., Santiago, B. X., Griffiths, R. E., Surma, P. 1996b, ApJSupp, 107, 1  
 Baade, W. 1957 in *Stellar Populations*, ed. O’Connell, D., p3 (Vatican Obs)

Balcells, M., & Peletier, R. F. 1994, AJ, 107, 135  
 Baugh, C. M., Cole, S., Frenk, C. S. 1996, MNRAS, 282, L27  
 Bouwens, R., Broadhurst, T., Silk, J. 1997, preprint astro-ph/9710291  
 Bower, R. G., Lucey, J. R., & Ellis, R. S. 1992, MNRAS, 254, 589  
 Bower, R. G., Kodama, T., & Terlevich, A. 1998. Preprint (astro-ph/9805290)  
 Brinchmann, J., Abraham, R. G., Schade, D., Tresse, L., Ellis, R. S., Lilly, S. J., Le Fevre, O., Glazebrook, K., Hammer, F., Colless, M., Crampton, D., & Broadhurst, T. 1998 (ApJ, in press, astro-ph/9712060).  
 Calzetti, D. 1997, AJ, 113, 162  
 Carney, B., Latham, D., & Laird, J. 1990. In ESO Proc., “Bulges of Galaxies”, eds. Jarvis, B., Temdrup, D.,  
 Charlot, S., & Bruzual, G. 1991, ApJ, 367, 126  
 Charlot, S., Worthey, G., & Bressan, A. 1996, ApJ, 457, 625  
 Charlot, S., & Bruzual, G. 1996, Documentation for GISSEL96 Spectral Synthesis Code.  
 Charlot, S., & Bruzual, G. 1998 (in preparation)  
 Cohen, J. G., Cowie, L. L., Hogg, D. W., Songaila, A., Blandford, R., Hu, E. M., & Shoptell, P. 1996, 471L, 5  
 Combes, F., Debbasch, F., Friedli, D., Pfeffinger, D. 1990, A&A, 233, 82  
 Connolly, A. J., Szalay, A. S., Dickinson, J., Subbararo, M. U., & Brunner, R. J. 1997, ApJ, 486L, 11  
 Cowie, L. L., Songaila, A., Hu, E. M., Cohen, J. G. 1996, AJ, 112, 839  
 Cowie, L. L., Hu, E. M., Songaila, A., Egami, E. 1997, ApJ, 481L, 9  
 de Jong, R. S. 1996, A & A, 313, 377  
 Dickinson et al. 1998, in preparation  
 Driver, S. P., Windhorst, R. A., Griffiths, R. E. 1995a, ApJ, 453, 48  
 Driver, S. P., Windhorst, R. A., Ostrander, E. J., Keel, W. C., Griffiths, R. E., Ratnatunga, K. U. 1995b, ApJ, 449, L23  
 Driver, S. P., Fernandez-Soto, A., Couch, W. J., Odewahn, S. C., Windhorst, R. A., Lanzetta, K., & Yahil, K. 1998 (ApJ(Letters), in press, astro-ph/9802092)  
 Eggen, O., Lynden-Bell, D., & Sandage, A. 1962, ApJ, 136, 748  
 Ellis, R. S. 1995 in IAU Symposium 164, ed van der Kruit, P. & Gilmore, G., 291  
 Ellis, R. S., Colless, M., Broadhurst, T., Heyl, J., Glazebrook, K. 1996, MNRAS, 280, 235  
 Ellis, R. S., Smail, I., Dressler, A., Couch, W. J., Oemler, A., Butcher, H., Sharples, R.M. 1997, ApJ, 483, 582  
 Ellis, R. S. 1997, ARA&A, 35, 389  
 Fomalont, E. B., Kellermann, K. I., Richards, E. A., Windhorst, R. A., & Partridge, R. B. 1997, ApJ, 475L, 5  
 Glazebrook, K., Abraham, R., Santiago, B., Ellis, R., Griffiths, R. 1997, preprint  
 Glazebrook, K., Ellis, R., Santiago, B., Griffiths, R. 1995a, MNRAS, 275, L19  
 Guhathakurta, P., Tyson, J. A., & Majewski, S. R. 1990, ApJLett, 357L, 9  
 Guzmán, R., Gallego, J., Koo, D. C., Phillips, A. C., Lowenthal, J. D., Faber, S. M., Illingworth, G. D., Vogt, N. P. 1997, ApJ, 489, 559  
 Hogg, D. W. et al. 1998. AJ (in press - astro-ph/980113)  
 Holtzman, J. A., Burrows, C. J., Casertano, S., Hester, J. J., Trauger, J. T., Watson, A. M., Worthey, G. 1995, PASP, 137, 1065  
 Kauffman, G., White, S. D. M., & Guiderdoni, B., 1993, MNRAS, 264, 201  
 Kauffmann, G., Charlot, S., & White, S. D. M. 1996, MNRAS, 283L, 117  
 Kormendy, J. 1992, in Proc.IAU Symp.153, “Galactic Bulges”, p.209, Kluwer, Dordrecht, eds. Dejonghe, H., Habing, H.  
 Kuijken, K., & Merrifield, M. R. 1995, ApJ, 443L, 13

- Lanzetta, K., M., Yahil, A., Fernandez-Soto, A. 1996, *Nature*, 386, 759
- Lilly, S. J., Cowie, L. L., & Gardner, J. P. 1991, *ApJ*, 369, 79
- Lilly, S. J., Schade, D., Ellis, R. S., Le Fevre, O., Brinchmann, J., Abraham, R., Tresse, L., Hammer, F., Crampton, D., Colless, M., Glazebrook, K., Mallen-Ornelas, G., Broadhurst, T. 1998 (*ApJ*, in press, astro-ph/9712061)
- Lilly, S., Le Fèvre, O., Hammer, F., Crampton, D. 1996, *ApJ* (Letters), 460, L1
- Lilly, S. J., Le Fèvre, O., Crampton, D., Hammer, F., Tresse, L. 1995a, *ApJ*, 455, 50
- Lilly, S. J., Tresse, L., Hammer, F., Crampton, D., Le Fèvre, O. 1995b, *ApJ*, 455, 108
- Lowenthal, J. D., Koo, D. C., Guzman, R., Gallego, J., Phillips, A. C., Faber, S. M., Vogt, N. P., Illingworth, G. D., & Gronwall, C. 1997, *ApJ*, 481, 673
- Madau, P. 1997, preprint, astro-ph/9707141
- Madau, P., Ferguson, H. C., Dickinson, M. E., Giavalisco, M., Steidel, C. C., Fruchter, A. 1996, *MNRAS*, 283, 1388
- Metcalf, N., Fong, R., Shanks, T., & Roche, N. 1995, *MNRAS*, 273, 257
- Meurer, G. R., Heckman, T. M., Lehnert, M. D., Leitherer, C., & Lowenthal, J. 1997, *AJ*, 114, 54
- Meurer, G. R., Heckman, T. M., Leitherer, C., Kinney, A., Robert, C., & Garnett, D. R. 1995, *AJ*, 110, 2665
- Menanteau, F., Ellis, R. S., Abraham, R. G., Barger, A., & Cowie, L. L. 1998, in preparation.
- Mobasher, B., Rowan-Robinson, M., Georgakakis, A., & Eaton, N. 1996, *MNRAS*, 282L, 7
- Norman, C. A., Sellwood, J. A., & Hasan, H. 1996, *ApJ*, 462, 114
- Odehahn, S. C., Windhorst, R. A., Driver, S. P., Keel, W. C. 1996, *ApJ* (Letters), 472, L13
- Pei, Y. C. 1992, *ApJ*, 395, 130
- Sandage, A. & Visvanathan, N. 1978 *ApJ*, 223, 707
- Schade, D. et al. 1998, in preparation
- Schade, D., Lilly, S. J., Crampton, D., Hammer, F., Le Fèvre, O., Tresse, L. 1995, *ApJ* (Letters), 451, L1
- Schmidt, M. 1968 *ApJ*, 151, 343.
- Shaw, M. 1993, *MNRAS*, 261, 718
- Smail, I., Hogg, D. W., Yan, L., & Cohen, J., *ApJ*, 449, 105.
- Stanford, S. A., Eisenhardt, P. R., & Dickinson, M. 1998, *ApJ*, 492, 461
- Tinsley, B.M. 1980 *ApJ*, 241, 41.
- van den Bergh, S., Abraham, R. G., Ellis, R. S., Tanvir, N. R., Santiago, B. X. 1996, *AJ*, 112, 359.
- Vogt, N. P., Forbes, D. A., Phillips, A. C., Gronwall, C., Faber, S. M., Illingworth, G. D., & Koo, D. C. 1996, *ApJ*, 465L, 15
- White, S. D. M. 1996, In *Science with Large Millimetre Arrays*, ed: Shaver, P., ESO Astrophysics Symposia (Berlin Springer), 33
- Williams et al. 1996, *AJ*, 112, 1335
- Zepf, S. E. 1997, *Nature*, 390, 377